

237-90

4/27/91
15P

NATURAL AND ORBITAL DEBRIS PARTICLES ON LDEF'S TRAILING AND FORWARD-FACING SURFACES

Friedrich Hörz

SN4, NASA / Johnson Space Center
Houston, Texas 77058
(713) 483-5042 / FAX (713) 483-5347

Ronald P. Bernhard

Lockheed Engineering & Science Co.
Houston, Texas 77058
(713) 483-5018 / FAX (713) 483-5347

Thomas H. See

Lockheed Engineering & Science Co.
Houston, Texas 77058
(713) 483-5027 / FAX (713) 483-5347

Donald E. Brownlee

Dept. of Astronomy; U. of Washington
Seattle, Washington 98195
(206) 543-8575 / FAX (203) 685-0403

ABSTRACT

Approximately 1000 impact craters on the Chemistry of Meteoroid Experiment (CME) have been analyzed by means of Scanning Electron Microscopy (SEM) and Energy Dispersive X-ray Analysis (EDXA) to determine the compositional make-up of projectile residues. This report completes our systematic survey of gold and aluminum surfaces exposed at the trailing-edge (A03) and forward-facing (A11) LDEF sites, respectively.

The major categories for the projectile residues were (a) natural, with diverse subgroups such as *chondritic*, *monomineralic silicates*, and *sulfides*, and (b) man made, that were classified into *aluminum* (metallic or oxide) and *miscellaneous* materials (such as stainless steel, paint flakes, etc). On CME gold collectors on LDEF's trailing edge ~11% of all craters >100 μm in diameter were due to man-made debris, the majority (8.6%) caused by pure aluminum, ~31.4% were due to cosmic dust, while the remaining 58% were indeterminate via the analytical techniques utilized in this study. The aluminum surfaces located at the A11 forward-facing site did not permit analysis of aluminum impactors, but ~9.4% of all craters were demonstrably caused by miscellaneous debris materials and ~39.2% were the result of natural particles, leaving ~50% which were indeterminate.

Model considerations and calculations are presented that focus on the crater-production rates for features >100 μm in diameter, and on assigning the indeterminate crater population to man-made or natural particles. An enhancement factor of 6 in the crater-production rate of natural impactors for the "forward-facing" versus the "trailing-edge" CME collectors was found to best explain all observations (*i.e.*, total crater number[s]), as well as their compositional characteristics). Enhancement factors of 10 and 4 are either too high or too low. It is also suggested that ~45% of all craters >100 μm in diameter are caused by man-made impactors on the A11 surfaces. This makes the production rate for craters >100 μm in diameter, resulting from orbital debris, a factor of 40 higher on the forward-facing sides as opposed to the trailing-edge direction.

INTRODUCTION

The "Chemistry of Micrometeoroids Experiment" (CME; ref. 1) exposed two substantially different collector materials to the hypervelocity particle environment on the Long Duration Exposure Facility (LDEF). The active experiment consisted of clamshell-type devices that could be opened and closed such that the collectors were protected against contamination during all ground handling and LDEF deployment. This instrument exposed ~0.82 m² of high-purity gold (>99.99% Au) on LDEF's trailing

414

edge (*i.e.*, Bay A03). The actual collectors consisted of seven individual panels (~20 x 57 cm each; ~0.5 mm thick). The Au collectors exhibited relatively low crater densities (refs. 1 and 2) because the trailing edge inherently yields the smallest particle flux (ref. 3) on a non-spinning platform, and because the collectors were only exposed for a total of 3.4 years (ref. 1). In contrast, the passive experiment continuously exposed, for 5.7 years, commercial grade aluminum surfaces (Al 1100 series, annealed, >99% pure Al) in the forward-facing, A11 location. Six individual panels (~41 x 46 cm, each; 3.2 mm thick) provided ~1.1 m² of cumulative surface area.

The purpose of CME was to obtain compositional information on the residues associated with hypervelocity craters. The present report complements earlier progress reports (refs. 1 and 2) primarily via analyzing additional craters on the A11 aluminum collectors. We now have systematically analyzed ~200 craters on the gold substrates and ~800 craters on the aluminum surfaces. The results refer to all craters above some arbitrary crater size on the respective host materials. Therefore, the findings will be representative for particles larger than some threshold size that impinge on the trailing-edge and forward-facing surfaces of a non-spinning spacecraft, such as LDEF, Mir or Space Station. Unquestionably, the current investigations are of a survey-type nature and remain incomplete in many detailed aspects. The current work primarily attempts to classify the particles into natural and man-made materials, and associated subclasses. Our analyses are qualitative, consistent with and sufficient for the above objectives. However, the presence of unmelted fragments within some of these craters permits -- in principle -- the determination of the detailed chemical and mineralogical make-up of some particles (refs. 2 and 4), as well as their isotopic characteristics (ref. 5) and potential organic-molecule content (ref. 6). However, such detailed analyses are so time consuming that they are not readily adapted to the characterization of entire populations of craters and projectiles (*e.g.*, refs. 4, 5, 6, 7 and 8).

We have analyzed 199 craters on the Au-collectors and 828 craters on four of the six A11 aluminum panels. In general, we followed the analytical procedures and compositional particle classifications developed during the analysis of interplanetary dust recovered from the stratosphere (refs. 9 and 10), or of space-retrieved surfaces such as Solar Maximum Mission replacement parts (refs. 11 and 12), or the Palapa satellite (ref. 13). The present effort specifically adds to these earlier analyses by characterizing a much larger number of events and by being able to place them into a dynamic dust environment, since LDEF was gravity-gradient stabilized, while all previously analyzed surfaces originated from spin-stabilized spacecraft. Unlike spin-stabilized satellites, LDEF offers the potential to yield substantial directional information (*e.g.*, refs. 3, 14, 15).

ANALYTICAL METHODS AND FINDINGS

Compositional analysis of projectile residues was conducted using an ISI-SR50 Scanning Electron Microscope (SEM), and a LINK eXL Energy Dispersive X-Ray (EDX) analyzer using a Si(Li) detector, arranged at 90° to the beam path. Although we characterize our analyses as qualitative and of a survey-type nature, we spent considerable efforts in optimizing the signal to noise ratio of the X-Ray spectra. Initially it was found that an uncomfortably large fraction of craters yielded spectra that contained no

detectable signal above that of the background. Therefore, we used a number of craters to investigate a range of electron-beam geometries (diameter and take-off angle), low- and high-beam voltage, and widely variable count times (minutes to hours). From these efforts it was determined that a relatively high-beam voltage (25-20 KeV) and long count times (500-1000 seconds) with the specimen tilted at 30° yielded the best results. It is our belief that high-beam voltages are best because the surface relief of the crater interiors tends to be uneven permitting excitation of more near-surface specimen volume compared to less penetrative, low-energy electrons. Count times in excess of 1000 seconds do not appreciably improve signal to noise ratios and do not warrant the additional expenditure of resources.

Contamination of our surfaces was not a significant problem because the composition of common contaminants differ dramatically from many projectile residues. Nevertheless, we have observed Si-Ca rich deposits in some crater interiors that, presumably, were derived from outgassed RTV (ref. 16). Interestingly, such deposits can have distinctly asymmetric distributions in some craters, substantiating the macroscopic LDEF observations of highly directional flow of gaseous contaminants and their condensates. We also observe some intrinsic, heterogeneously distributed contaminants, the result of manufacturing procedures in our collector materials, most notably as in the gold and Si in the aluminum. The anodized layer on the aluminum surfaces varied from plate to plate, but background from this source was taken into consideration. On the A11 aluminum plate E00H every crater analyzed contained significant amounts of Si, Mg, and Fe, as well as other contaminants to the degree that none of these craters was used in the particle population studies below (*i.e.*, these craters were excluded from this report).

The sources for colliding projectiles in low-Earth orbit (LEO) are either “natural” or “man-made”. The natural particles encountered are described as micrometeoritic, cosmic dust, or interplanetary dust, and originate from either comets or asteroids (ref. 10). The man-made particles result from explosions and collisions, and the associated fragmentation products of satellites, solid rocket burns, ablation of thermal coatings from small particle collisions, atomic oxygen erosion, and human waste dumped in LEO (ref. 14).

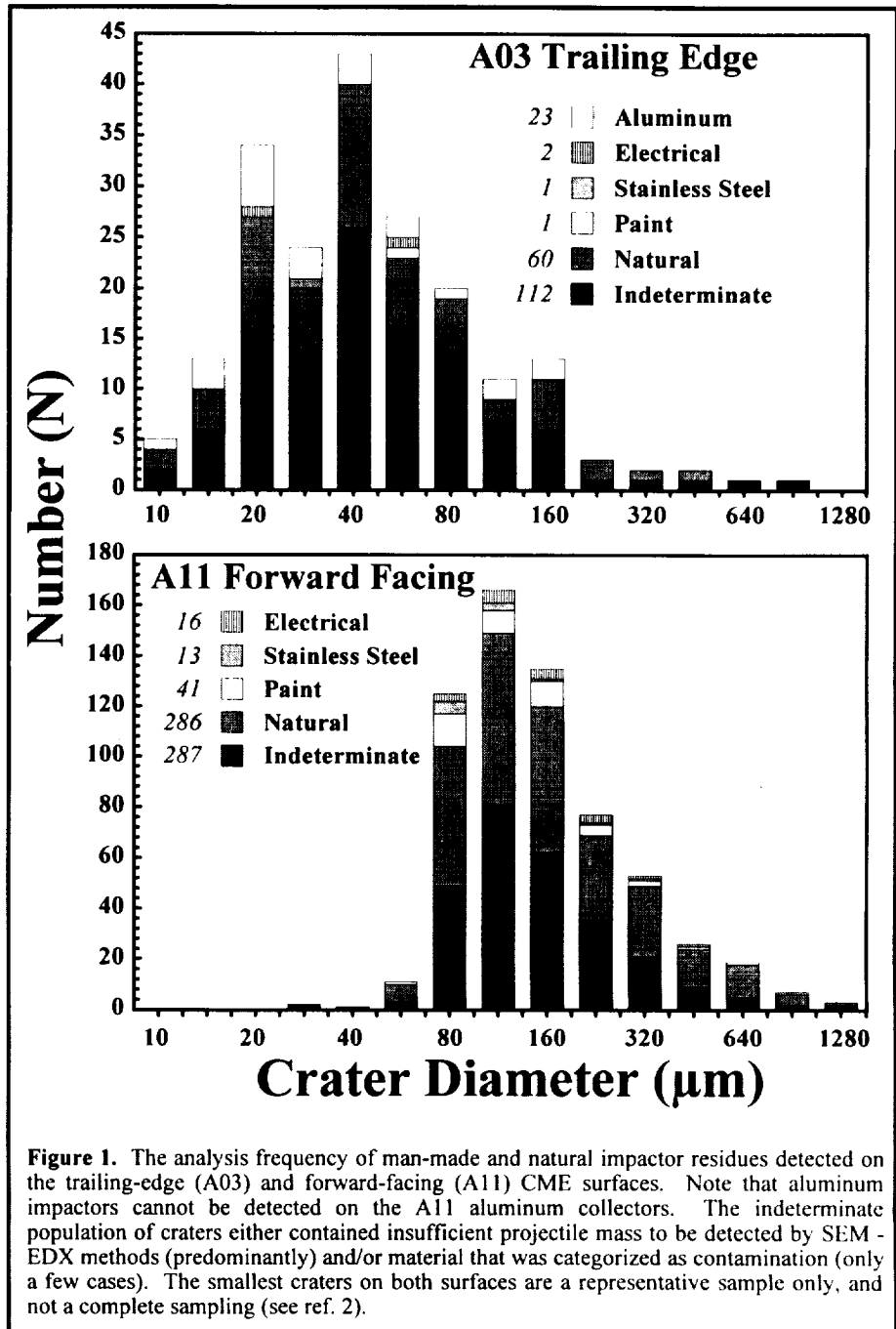
“Natural” particles can be subdivided into (1) chondritic, that are largely made up of relatively well-mixed and homogenized, fine-grained matrices. (2) Monomineralic silicates, characterized by high concentrations of Si, Mg, and Fe; these particles are mostly found in molten form, but on occasion unmelted fragments of olivine and pyroxene are preserved. (3) Fe-Ni-sulfide rich particles are found, yet only as melts; these particles are frequently associated with minor chondritic melts/glasses, suggesting that large Fe-Ni sulfides grains, common in meteorites, had some fine-grained chondritic matrix attached to them.

The “orbital-debris” impacts contained (1) Fe-Ni-Cr rich particles representing stainless steel, (2) Zn-Ti-Cl rich residues characteristic of thermal protective spacecraft paints, (3) Ag, Cu, or Pb-Sn rich residues originating from solar cells or other electrical components of spacecraft hardware, and (4) particles that contain aluminum only, without specifying whether they were metallic or oxidized. Obviously such aluminum impactors could only be detected on the gold collectors and their occurrence on the forward-facing aluminum substrates is not amenable to direct compositional analysis. Throughout this report, the above category 1-3 particles will be referred to as “miscellaneous” debris, as opposed to the pure “aluminum” particles of category 4.

For many individual craters one may obtain x-ray spectra that reflect specific component minerals of natural dust grains (*e.g.*, olivines or pyroxenes) and their mixtures. However, variability within the pure crater melts was observed as well, with the largest variations occurring in those craters that contained unmelted residues, suggesting the presence of incompletely mixed mineral melts (refs. 17 and 18). Generally, this melt variability relates to subtly different elemental ratios among different spectra obtained from the same specimen. Nevertheless, this specimen heterogeneity is slight and does not affect our classification into natural and man-made particle sources.

RESULTS

Most summarizing figures in this report are updates of our earlier progress report (ref. 2), with minor modifications in substance, yet with increased statistical significance. Figure 1 summarizes all analyses to date and plots the number-frequency of recognized projectile types versus crater size. The intent is to illustrate the relative frequencies of the major particle types. We conclude from Figure 1 that the majority of craters that contain identifiable residues were caused by natural, cosmic-dust particles accounting for ~68% on the gold and 77% on the aluminum collectors. It is equally important to note that ~50% of all craters did not contain sufficient residue mass to be analyzed by our SEM methods (also see refs. 2, 5, 7 and 8). Most likely these structures are a velocity-biased set of craters with encounter velocities sufficiently high to eject most or all of the projectile melts from the growing crater cavity (ref. 19), if not as vapors



(e.g., refs. 2 and 5), or they are the result of unusual projectile properties (e.g., highly porous, low-density particles ?) that are easily vaporized.

The man-made sources are totally dominated by aluminum particles on the trailing-edge gold surfaces, (i.e., 23 aluminum particles versus 4 miscellaneous impactors). Note, however, that the forward-facing A11 aluminum collectors do not permit recognition of aluminum and all man-made particles on these detectors are of the “miscellaneous” category, essentially by definition. These include 41 paint flakes, 13 stainless-steel particles and 16 fragments of electrical components on components E00E, E00F and E00G. In particular, note the dominance of paint flakes on the forward-facing surface (41 craters), whereas only 1 paint flake was identified on the trailing edge.

Other investigators (refs. 4, 5, 6, 7 and 8) have analyzed projectile residues associated with LDEF craters from various surfaces and their results are consistent with those observed on the CME collectors. Specifically, the somewhat surprising presence of man-made impactors on the trailing edge (ref. 1, 2 and 15) was confirmed by others (ref. 8).

The size distribution of the crater populations that were analyzed on the two collector surfaces differed in that all craters $>30 \mu\text{m}$ and $>75 \mu\text{m}$ in diameter on the gold and aluminum surfaces, respectively, were investigated. Smaller craters which appear in the data are merely representative of the small crater population. In addition, the absolute number of craters larger than some given size depends on total exposure time of the two collector surfaces (i.e., 3.5 years for the gold and 5.7 years for the aluminum surfaces [ref. 1]). Therefore, it is not possible to directly compare the analysis frequencies of the forward-facing and trailing-edge surfaces as illustrated in Figure 1. It is much more instructive to consider crater-production rates as illustrated in

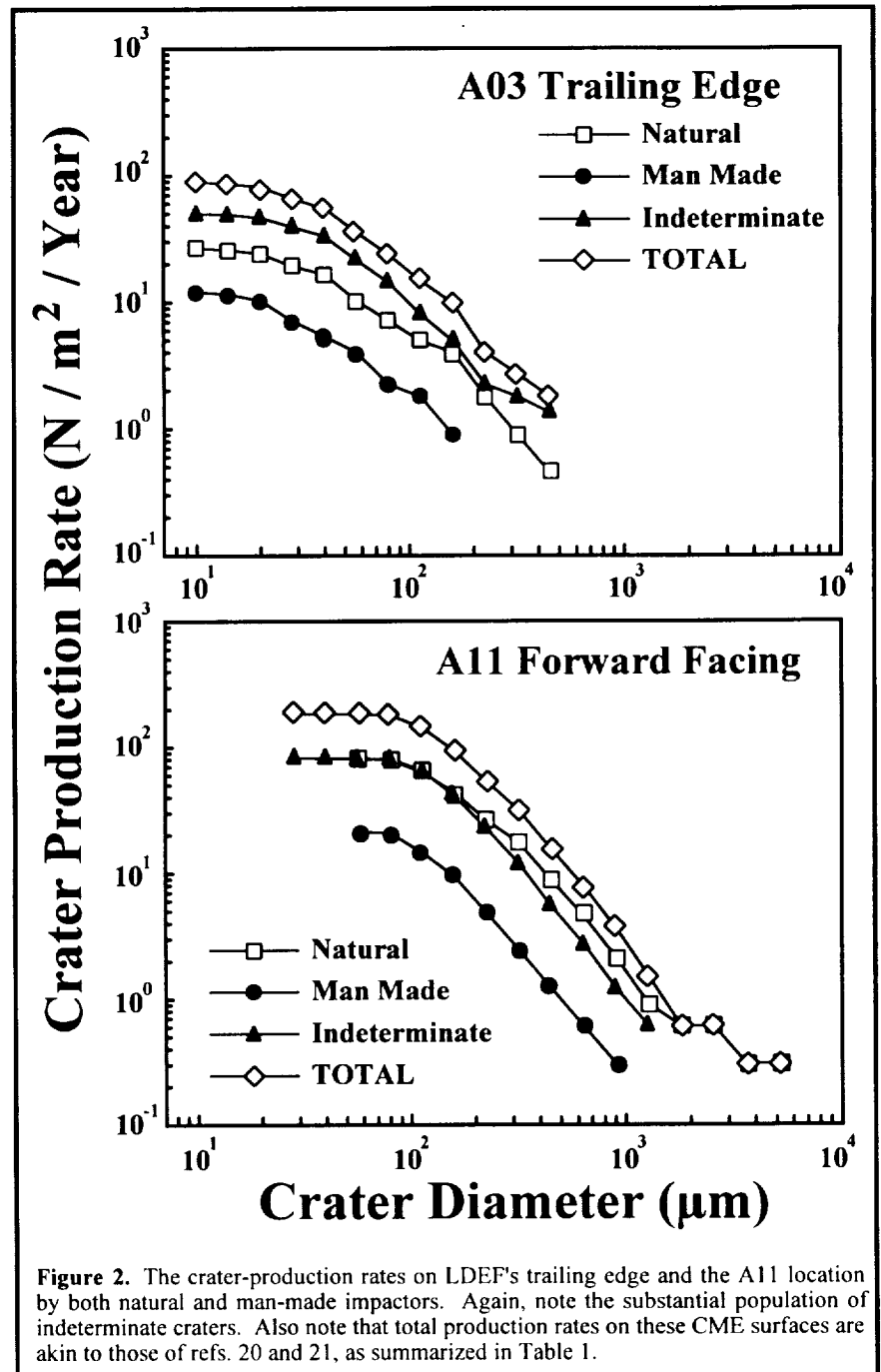


Figure 2, which corrects for different exposure histories and permits for direct comparison of identical crater sizes (e.g., ref. 3). Note again the unfortunately large fraction of indeterminate craters/projectiles and the inability to analyze for aluminum particles on the aluminum collectors. Also, subtle changes in slope (i.e., relative size frequency) are observed for the different crater classes, yet such differences are not statistically significant; for clarity, we avoided statistical error bars on these cumulative plots.

Table 1 lists specific crater-production rates that were extracted from Figure 2 and compares them with the crater-production rates of Humes (ref. 20 and 21) and See *et al.* (ref. 22). For the A03 orientation our total crater-production rates are in excellent agreement with those of others, yet this is somewhat fortuitous considering the vastly different collector substrates (i.e., gold versus aluminum). The forward-facing surfaces were all composed of anodized aluminum, 6061-T6 in the case of Humes and See *et al.* and 1100 series aluminum for the CME surfaces. Agreement among Humes and See *et al.* is good at all sizes, as is the CME production rate for craters >1000 μm in diameter; the CME data from 100 μm to 500 μm in diameter are modestly higher than those of Humes or See *et al.* by as much as ~20%. While this difference is substantial, it is still within statistical uncertainty. Our lower CME numbers at the 50 μm size range are clearly the consequence of incomplete sampling for craters <75 μm in diameter on our aluminum plates.

Table 1. Crater-production rates ($\text{N}/\text{m}^2/\text{y}$) for select crater sizes on CME's trailing-edge (A03) gold surfaces and the forward-facing (A11; 52° off of LDEF's leading edge) aluminum collectors.

	CRATER DIAMETER (μm)				
	>10	>50	>100	>500	>1000
TRAILING EDGE (A03)					
Total Population					
Humes (1994)	?	39	20	1.6	0.28
See <i>et al.</i> (1994)	60	31	17	1.5	?
This Work	90	41	17.5	1.8	?
Natural		26	11.2	5.5	0.41
Man Made		11.5	4.6	1.9	<0.1
Miscellaneous	1.2	0.7	0.4	?	
Aluminum	10.3	3.9	1.5	<0.1	
FORWARD FACING (A11)					
Total Population					
Humes (1994)		290	145	9.2	2.9
See <i>et al.</i> (1994)		280	137	7.9	1.6
This Work		185	168	12.4	2.75
Natural		81	66	5.3	0.97
Man Made		?	?	?	?
Miscellaneous		20.5	15.8	0.92	0.25
Aluminum		?	?	?	?

The detectors of refs. 20, 21 and 23 were fabricated from aluminum 6061-T6 which differs in strength properties (e.g., refs. 19 and 23) from our 1100 aluminum. However, the difference between aluminum 6061 and 1100 is relatively subtle, in the context of Table 1, based on cratering theory (refs. 19, 23) and empirical crater-shape measurements on LDEF surfaces (ref. 24). Also note the differences between Humes and See *et al.* for identical materials. In addition, all aluminum surfaces of Table 1 were anodized; the oxide layer which results from anodizing has demonstrably affected many of the small craters in our 1100 Al-alloy collector. Despite its high density, gold is so ductile that the crater size resulting from a

given projectile (ref. 1) is (fortuitously) similar to that of aluminum (ref. 19, 23). Very generally speaking, our total crater-production rates for the A11 and A03 locations are consistent with the observations of others. Furthermore, the total crater-production rate on the CME surfaces is a factor of ~5-7 higher (depending on specific size; see Table 1) on the forward-facing surfaces compared to the trailing-edge direction.

What is new and unique to the present work is that we can assign specific impactor compositions and origins to ~50% of these craters. Those produced by natural impactors are more frequent than orbital-debris craters at all crater diameters analyzed. Typically, cosmic-dust craters outweigh those produced by orbital-debris particles by 2:1 (see Table 1). The production rate of natural cratering events is a factor of 6-10 higher for the A11 direction compared to the A03 location, consistent with (ref. 3).

INTERPRETATIONS

Particle Frequency And Fluxes

As previously discussed in our earlier report (ref. 2), the most general and useful way to characterize the hypervelocity environment in space is on a particle-size or mass basis. This conversion from crater diameter to particle size will be the subject of this section. Particle size and mass not only relate directly to a particle's origin and formative processes, but it is the only way of assigning some kinetic energy, at a given model velocity, to a single particle or to some population of particles when estimating collisional damage and risks under generalized conditions. The conversion of a measured crater diameter to some projectile size and mass is a crucial part of LDEF cratering studies, and the most critical one for collisional risk assessment and management. However, we remind the general reader, as well as some of our peers, that the conversion of a crater diameter to particle mass is not possible at present without substantial model assumptions.

Our major assumptions are as follows (see ref. 2 for details). Principally, we used the cratering equations for aluminum of ref. 23, and our own, dedicated experiments in gold (ref. 1) as the basic empirical insights. Use of Ref. 19 would yield essentially identical results. Projectile velocities, normal to the collector surface, were adopted from Zook (ref. 3) and Kessler (ref. 15) for natural and man-made debris, respectively. We used 12 km/s and 1.75 km/s for natural and man-made particles respectively on the trailing-edge collectors and 17.9 km/s (natural) and 7.8 km/s (man-made) for the A11 aluminum surfaces. Projectile density for all impactors was assumed to be 2.7 g/cm³. Most of these assumptions are well constrained except density, which will have substantial effects (refs. 19 and 23; *i.e.*, factors of 3-5 in resulting projectile masses for a reasonable range of densities).

The resulting projectile sizes and their fluxes are presented in Figure 3, along with the crater production rates from Figure 2. Obviously, only those craters which have identified projectile residue can be considered for such a plot, because their man-made versus natural origin provides the impact velocity in the cratering equations; by definition, indeterminate craters possess unknown encounter velocities and

require additional assumptions (see below) to be converted into associated impactors. Projectile calibration simply solves for some *velocity dependent* constant with which the crater diameter relates to the impactor ($D_{\text{crater}}=K \cdot D_{\text{impactor}}$). At unit crater size fast natural impactors are substantially smaller than the comparatively slow man-made particles. The conversion from crater diameter to projectile size can lead to seemingly confusing results. Note that the man-made craters are less abundant than natural ones on the trailing edge, yet on a projectile-size basis, the reverse applies, and man-made particles (of very slow velocity) become more abundant than (high velocity) cosmic dust.

Thus, we re-emphasize (see ref. 2) that great care is necessary when discussing the absolute and relative frequency of man-made versus natural particles on LDEF. Substantially different absolute and relative frequencies may result, depending on whether one argues from an analysis frequency basis

(Figure 1), from a crater-productions rate (Figure 2), or from a particle-flux basis (Figure 3). Crater and projectile sizes relate to each other via a velocity dependent constant. Consequently, the absolute and relative frequencies of crater diameters and projectile sizes will shift different amounts (Figure 3) if they are the result of impactors with systematically different velocities.

Table 2 summarizes the observed fluxes for some typical projectile sizes of natural and man-made particles. Debris dominates (by some factor of 3) the population for particles $>100 \mu\text{m}$ in diameter on the trailing edge, whereas natural particles seem to become increasingly more populous with decreasing particle size; man-made debris and natural dust occur in similar proportions at particle sizes $<50 \mu\text{m}$ in diameter and cosmic dust becomes dominant at particle diameters of $<10 \mu\text{m}$ on the trailing edge. Not very much can be demonstrated for the forward-facing A11 surfaces, other than that natural particles dominate the miscellaneous debris category at all sizes, typically by factors of 2-3. Furthermore, the ratio between forward-facing A11 surface and the A03 trailing-edge surface is $\sim 5-6$ for natural particles of all

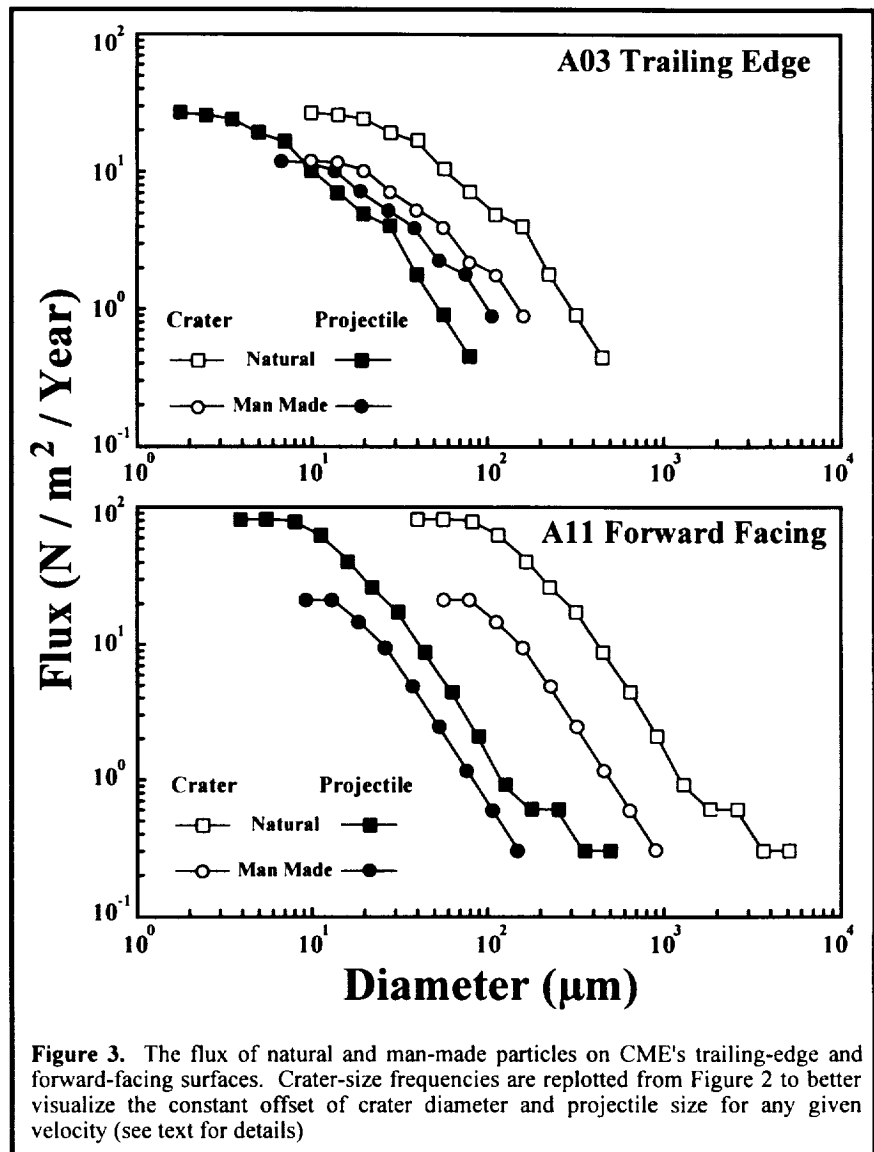


Figure 3. The flux of natural and man-made particles on CME's trailing-edge and forward-facing surfaces. Crater-size frequencies are replotted from Figure 2 to better visualize the constant offset of crater diameter and projectile size for any given velocity (see text for details)

sizes. We did not observe size-dependent effects among the natural impactors between our forward-facing and trailing-edge viewing directions.

We again reemphasize the fact that we could not detect man-made aluminum particles on the A11 surface; this restricts our comparisons of forward-facing and trailing-edge surfaces to the miscellaneous debris category. The latter has an enhancement factor of ~20 on the forward-facing side for small particles (~10 μm in diameter) and a factor of ~7 for particles > 50 μm in diameter. At face value this argues for variable size-frequency distributions of the miscellaneous debris category, with small particles being relatively more abundant in the forward-facing directions.

Table 2. Flux (N/m²/Year) of known particles of select sizes on CME's trailing-edge (A03) and forward-facing (A11) collector surfaces.

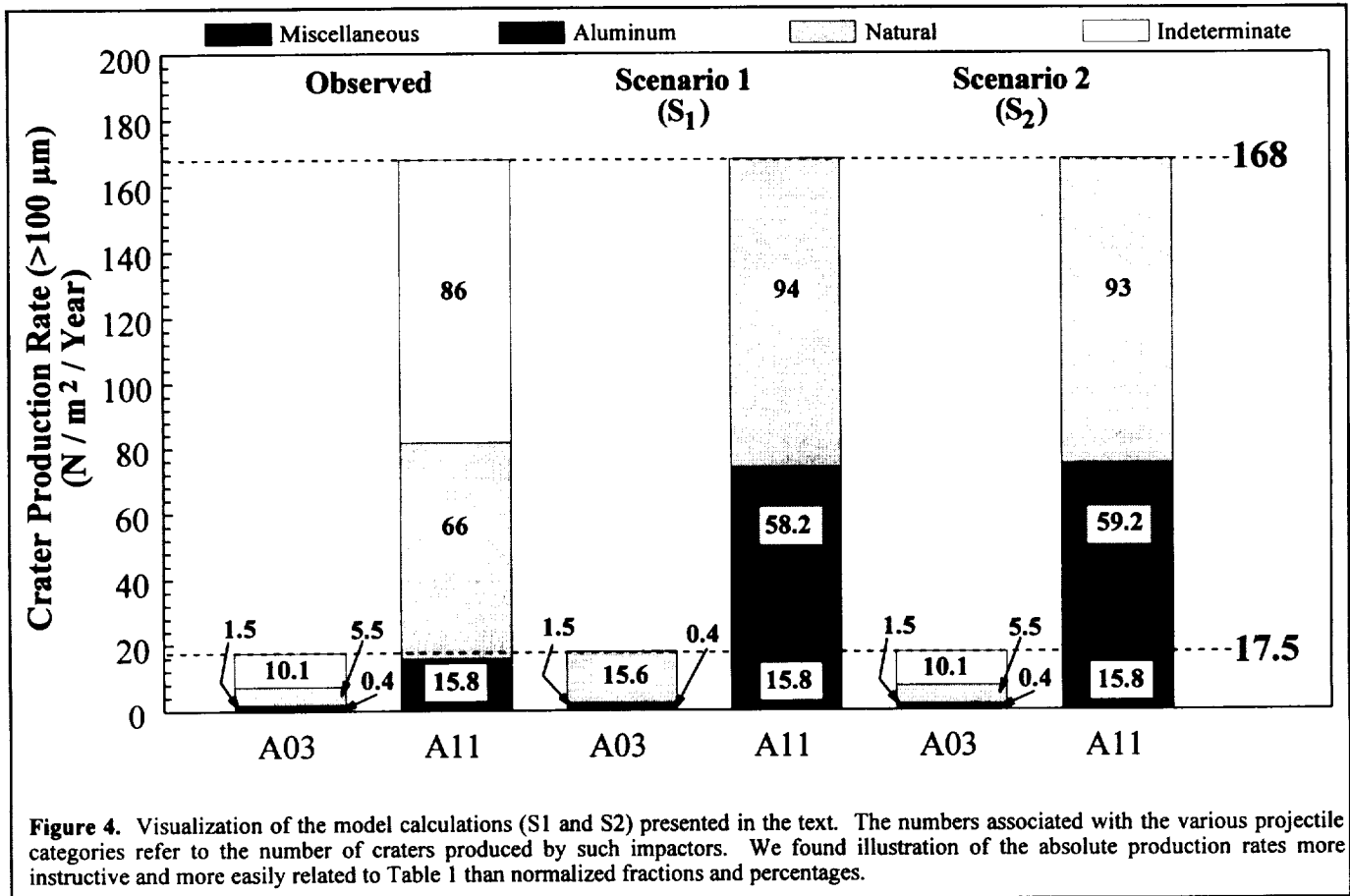
	PARTICLE DIAMETER (μm)				
	>5	>10	>50	>100	>500
TRAILING EDGE (A03)					
Natural	20.5	10.1	1.2	0.29	<0.1
Man Made	14	11.2	2.5	0.98	<0.1
Miscellaneous	1.6	1.2	0.4	?	
Aluminum	12.4	10	2.1	0.98	
FORWARD FACING (A11)					
Total Population					
Natural	82	66	7	1.65	0.27
Man Made		?	?	?	?
Miscellaneous	?	22	2.8	0.68	<0.1
Aluminum		?	?	?	?

The Indeterminate Crater Population

The presence of orbital-debris particles on the trailing edge of LDEF was unexpected (ref. 1). These findings were subsequently modeled by Kessler (ref. 15) who demonstrated that (1) only sources in highly elliptical orbits can account for debris on LDEF's trailing edge and (2) these sources were vastly underestimated previously as contributors to the man-made particle environment. Having now a complete and much more comprehensive database, we will re-examine those assumptions used by Kessler that specifically revolve around the possible assignment of the substantial indeterminate crater population to either natural or man-made impactors.

In evaluating the relative roles of natural and man-made impactors we heavily rely on the trailing-edge gold surfaces, where analytical conditions were more favorable, having a >99.99% pure Au substrate. We also use our total crater-production rates (that agree with others [refs. 20, 21 and 22]) to form rigorous constraints on the total crater population; the CME rates (Table 1) are modestly higher than those of Humes and See *et al.*, and neither of our scenarios (presented below) will tolerate the formation of additional craters. Two scenarios are presented, labeled S₁ and S₂ in Figure 4. The first scenario (S₁) assumes that *all* indeterminate craters on the trailing-edge gold surfaces are caused by natural dust particles, due to their high encounter velocities and associated loss of impactor. All debris impacts occurred at very low speeds on the gold and should be quantitatively accounted for, as well as categorized

as either aluminum or miscellaneous debris. In addition, we postulate that the crater-production rate by cosmic-dust particles (ref. 3) on the forward-facing surface ($\sim 52^\circ$ off the actual leading edge) is a factor of 6 higher than on the trailing edge. Scenario 2 (S_2) follows Ref. 15 and transfers the relative frequency of aluminum and miscellaneous debris materials of the trailing-edge gold collector to the forward-pointing aluminum surfaces.



Results of these model calculations are visualized in Figure 4, using the observed production rates for craters $>100 \mu\text{m}$ in diameter. This diameter was chosen as being well (best) represented on both CME surfaces. We note that Scenario 1 yields a total of 94 natural craters (15.6×6), which compares to the 66 identified craters. This relegates the remaining ~ 74 craters ($168-94$) as being man-made, 16 of which are known to have resulted from miscellaneous debris materials. This leaves 58 craters ($74-16$) in the pure aluminum category for the A11 surface, and an $\sim 3.6:1$ ratio ($58:16$) of aluminum to miscellaneous debris. The overall ratio of man-made to natural dust impacts in Scenario 1 is $(74:94) \sim 0.79$ for the forward-facing orientation. Thus, for the A11 location $\sim 55\%$ of all craters seem to be due to natural impactors, $\sim 35\%$ are due to pure aluminum particles and $\sim 10\%$ are caused by miscellaneous debris.

The main feature of Scenario 2 is to first associate a complement of indeterminate craters on the A11 site with a debris origin. We have done this by transferring the observed crater-production ratio of ~ 3.75 for aluminum and miscellaneous particles ($1.5:0.4$; see Table 2) from the trailing edge to the forward-facing location. Using the above ratio, one associates with the 15.8 miscellaneous craters (15.8×3.75) a total of 59 aluminum craters for A11. This result is virtually identical with Scenario 1, albeit by totally

fortuitous coincidence. It nevertheless shows that the two dramatically different scenarios yield results that seem compatible with the observed crater populations. However, two caveats apply to the detailed numbers:

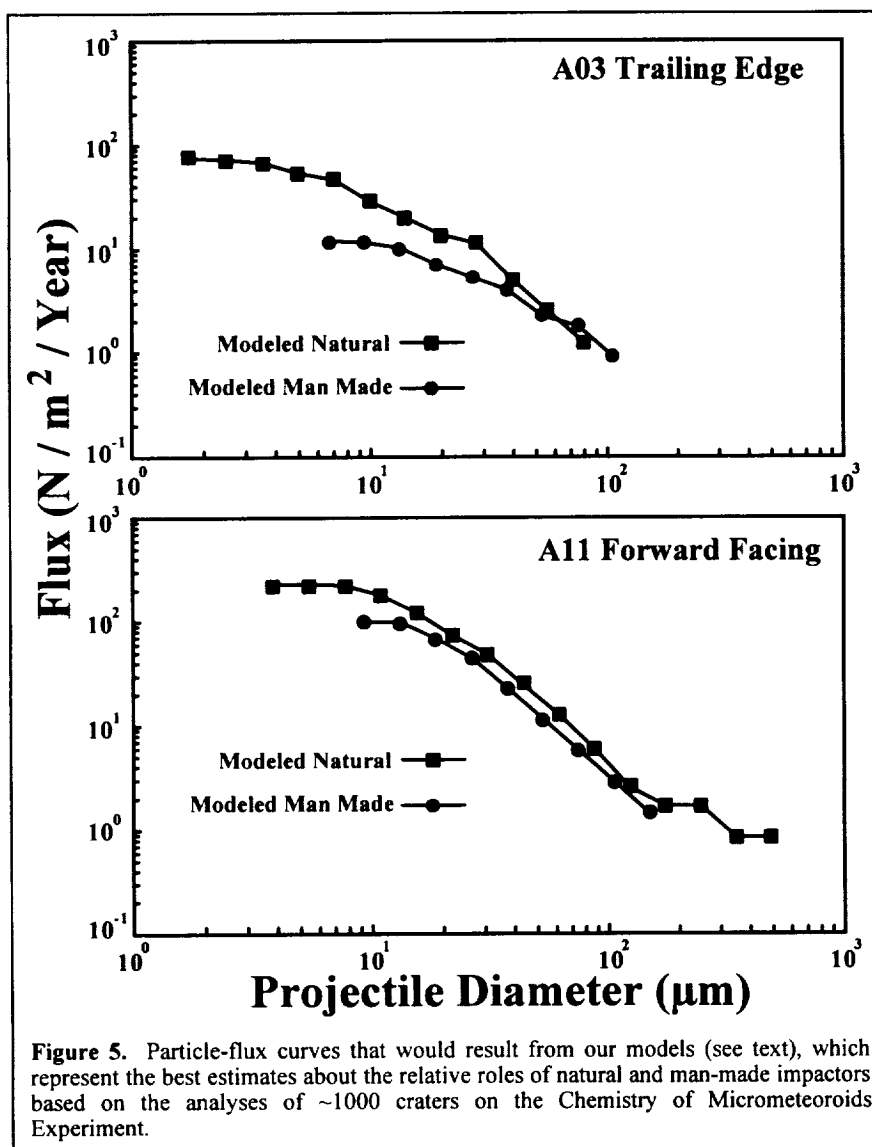
- 1) Note that our production rate of 168 craters on the A11 surface is somewhat higher than the values (~140) of Refs. 20, 21 and 22. The latter values could only be accommodated by substantially decreasing the aluminum projectiles (from 58 to ~30) in Scenario 1, and by decreasing the natural impactors from 93 to 65 in Scenario 2. The point here is that relatively modest changes in the total crater-production rate can precipitate substantial changes in the relative frequency of man-made versus natural impactor population(s) observed by CME.
- 2) Scenario 1 totally depends on the enhancement factor of 6 in the crater-production rate between trailing-edge and forward-facing LDEF orientations. Note that our own (Table 1) enhancement factor for craters >100 μm in diameter is 9.6 (168:17.5). This factor results in a total of 150 natural impacts (15.6 x 9.6) for Scenario 1, and leaves virtually no room for aluminum impactors. As a result, we suggest that an enhancement factor of 10 is too high. On the other hand, an enhancement factor of 4 between trailing edge and the A11 forward-facing surface seems too low for natural particles, because not enough natural craters would result (*i.e.*, 15.6 x 9.6 = 62, yet 66 craters were observed). Note that Scenario 2 is unaffected by this consideration.

Based on the foregoing we conclude that the indeterminate crater population on the trailing edge could be entirely caused by cosmic-dust impacts, whereas that of the forward-facing surface represents a mixture of man-made and natural impactors. Total average fraction of man-made versus natural craters is 0.109 (1.9:17.5) for the trailing edge and 0.44 (74:168) for the forward-facing A11 location. The trailing edge crater-production rate by natural particles seems enhanced by some factor of 6 on the A11 versus the A03 surface; enhancement factors of 10 seem too high, while 4 seem too low to accommodate the compositional observations. Any enhancement factor between 5 and 8 is viable, yet any specific value will precipitate very specific particle populations that differ from those advocated and preferred here.

It must be emphasized again that the above conclusions are valid only for craters >100 μm in diameter. Note in Table 2 the steady increase of aluminum impactors in the population of small craters. The aluminum to miscellaneous debris ratio is 3.75 (1.5:0.4) for >100 μm in diameter particles, 5.6 (3.9:0.7) for >50 μm in diameter particles and 8.6 (10.3:1.2) for the >10 μm in diameter particles. Therefore, it seems difficult to infer the relative frequencies of natural versus man-made impactors at millimeter scales.

While we have argued above that particle diameter or mass are the only proper way to ultimately compare and quantify the different impactor populations, this can be done at present only with craters containing identifiable residues, such as in Figure 3 and Table 2. Deconvolution of the indeterminate crater population into man-made and natural particles differs from the above considerations of crater-production rates. The latter benefits from having the total observed crater population as a firm upper limit and constraint. Because crater diameter depends on both particle size and velocity, repetitive iterations will be needed to approximate the actual fractions of man-made and natural impactors responsible for the indeterminate crater category. Such calculations exceed the scope of this report.

For the time being we use the above crater-production rates and suggest that the particle flux for man-made objects in Figure 3 is essentially correct for the trailing-edge surfaces, and that the natural flux should be increased by some factor of 2.8 ($15.6_{\text{natural modeled}}:5.5_{\text{natural observed}}$). By the same token, the flux on A11, following the S1 scenario, should be increased by factors of 1.4 ($94_{\text{natural, modeled}}:66_{\text{natural, observed}}$) for natural impactors, relative to Figure 3. Scenarios 1 and 2 leave the miscellaneous debris category essentially untouched and largely deal with the missing aluminum category on A11. The aluminum particle flux on A11 is a factor of 3.75 ($59_{\text{aluminum, modeled}}:15.8_{\text{miscellaneous, observed}}$) higher than the miscellaneous flux in Figure 3. Our modeled fluxes are summarized in Figure 5. These fluxes represent the best estimates about the relative roles of natural and man-made impactors that could be extracted from the analysis of ~1000 craters on the Chemistry of Micrometeoroids Experiment.



CONCLUSIONS

We have characterized chemically and qualitatively the projectile residue remaining in ~1000 individual craters on the Chemistry of Micrometeoroid Experiment, representing the trailing edge and a forward-facing direction (A11; ~52° off the plane of orbital motion) of the LDEF satellite. The production rate of impact craters >100 µm in diameter and ~50 µm deep (see ref. 24) due to natural particles is a factor of 6 higher in the forward-facing direction compared to the trailing edge. The population consists, in decreasing abundance, of particles with chondritic bulk compositions, followed by mafic silicates (olivine; pyroxene) and Fe-Ni-rich sulfides. Man-made impactors are dominated by pure aluminum particles; a substantial population of paint flakes impinges preferentially on the front surfaces, while steel particles and

fragments of electronic devices are significant as well. The production rate of craters >100 µm in diameter by man-made impactors is approximately half that of natural particles in the forward-facing (A11)

direction, and ~10% for the trailing edge. The absolute difference in the crater-production rate by man-made impactors is a factor of ~40 between trailing and forward-facing pointing directions of LDEF.

Although the activity of man-made impactors on the trailing edge is modest, it was nevertheless unexpected and has already lead to some revision of the particulate environment in LEO (ref. 15). The present report provides the statistically most significant compilation of particle compositions to date. It will hopefully assist in the further refinement of environmental models and the associated collisional hazard.

REFERENCES

- 1) Hörz, F., Bernhard, R.P., Warren, J., See, T.H., Brownlee, D.E., Lurance, M.R., Messenger, R., and Peterson, R.P. (1991) Preliminary Analysis of LDEF Instrument A0187-1 Chemistry of Micrometeoroids Experiment", *LDEF - 69 Months in Space, First Post-Retrieval Symposium, NASA CP-3134*, p. 487-501.
- 2) Bernhard, R.P., See, T.H. and Hörz, F. (1993) Projectile Compositions and Modal Frequencies on the "Chemistry of Micrometeoroids" LDEF Experiment., *LDEF - 69 Months in Space, Second Post Retrieval Symposium, NASA CP 3194*, p.551-573.
- 3) Zook, H. A. (1991) Deriving the Velocity Distribution of Meteoroids from The Measured Meteoroid Impact Directionality on the Various LDEF Surfaces, *LDEF - 69 Months in Space, First Post-Retrieval Symposium, NASA CP-3134*, p. 569-579.
- 4) Brownlee, D.E., Joswiak, D., Bradley, J., and Hörz, F. (1993) Interplanetary Meteoroid Debris in LDEF Metal Craters, *LDEF - 69 Months in Space, Second Post-Retrieval Symposium, NASA CP-3194*, p.577-584.
- 5) Amari, S., Foote, J., Swan, P., Walker, R.M., Zinner, E., and Lange, G. (1993) SIMS Chemical Analysis of Extended Impacts in the Leading and Trailing Edges of LDEF Experiment A0231-2, *LDEF - 69 Months in Space, Second Post-Retrieval Symposium, NASA CP 3194*, p. 513-528.
- 6) Bunch, T.E., Radicati di Brozolo, F., Fleming, R.H., Harris, D.W., Brownlee, D.E. (1992) LDEF Impact Craters formed by Carbon-Rich Impactors: a Preliminary Report, *LDEF - 69 Months in Space, First Post-Retrieval Symposium, NASA CP 3134*, p. 549-564.
- 7) Simon, C.G., Hunter, J.L., Griffis, D.P., Misra, V., Ricks, D.A., Wortmann, J.J., and Brownlee, D.E. (1993) Elemental Analyses of Hypervelocity Microparticle Impact Sites on Interplanetary Dust Experiment Sensor Surfaces, *LDEF - 69 Months in Space, Second Post-Retrieval Symposium, NASA CP 3194*, p. 677-692.

- 8) Mandeville, J.C. and Borg, J. (1991) Study of Dust Particles On-Board LDEF: The FRECOPA Experiments A0138-1 and A0138-2, *LDEF - 69 Months in Space, First Post-Retrieval Symposium, NASA CP-3134*, p. 423-434.
- 9) Zolensky, M.E. ed. (1990), Particles from Collection Flag L2405, *Cosmic Dust Catalog, 11, 1, JSC #24461-SN-83*, 170 pp.
- 10) Brownlee, D.E. (1985) Cosmic Dust: Collection and Research, *Ann. Rev. Earth. Planet. Sci.*, 13, p. 134-150.
- 11) Warren, J.L., Zook, H.A., Allton, J.H., Clanton, U.S., Dardano, C.B., Holder, J.A., Marlow, R.R., Schultz, R.A., Watts, L.A., and Wentworth, S.J. (1989) The Detection and Observation of Meteoroid and Space Debris Impact Features on the Solar Max Satellite, *Proc. Lunar Planet. Sci. Conf.*, 19th, p. 641-657.
- 12) Rietmeijer, F.J.M., Schramm, L., Barrett, R.A., McKay, D.S., and Zook, H.A. (1986) An Inadvertent Capture Cell for the Orbital Debris and Micrometeoroids; the Main Electronic Box Thermal Blanket of the Solar Maximum Satellite, *Adv. Space Res.*, 6, p. 145-149.
- 13) Bernhard, R.P. (1990) *Impact Features on Returned Palapa Hardware*, Internal NASA Report.
- 14) Kessler, D.J., Reynolds, R.C. and Anz-Meador, P.D. (1988) *Orbital Debris Environment for Spacecraft Designed to Operate in Low Earth Orbit, NASA TM-100 471*.
- 15) Kessler, D. J. (1992) Origin of Orbital Debris Impacts on LDEF'S Trailing Surfaces, in *LDEF - 69 Months in Space, Second Post-Retrieval Symposium, NASA 3194*, p.585-594.
- 16) Crutcher, E.R., Nishimura, L.S., Warber, K.J., and Wascher, W.W. (1991) Migration and Generation of Contaminants From Launch through Recovery: LDEF Case History, in *LDEF - 69 Months in Space, First Post-Retrieval Symposium, NASA CP-3134*, p. 125-140.
- 17) Schaal, R.B., Hörz, F., Thompson, T.D. and Bauer, J.F. (1979) Shock Metamorphism of Granulated Lunar Basalt, *Proc. Lunar Planet. Sci. Conf.*, 10th, p. 2547-2571.
- 18) Stöffler, D. (1972) Deformation and Transformation of Rock-Forming Minerals by Natural and Experimental Shock Processes; Behavior of Minerals under Shock Compression, *Fortschr. Mineral.*, 49, p. 50-113.
- 19) Watts, A., Atkinson, D. and Rieco, S. (1993) Dimensional Scaling for Impact Cratering and Perforation, *NASA Contractor Report NCR 188259*, 160 pp.
- 20) Humes, D.H. (1992) Large Craters on the Meteoroid and Space Debris Impact Experiment, in *LDEF - 69 Months in Space, First Post-Retrieval Symposium, NASA CP-3134*, p. 399-422.

- 21) Humes, D. (1994) Small Craters on the Meteoroid and Space Debris Experiment. *LDEF - 69 Months in Space, Third LDEF Post-Retrieval Symposium, NASA CP-3275*, this volume.
- 22) See, T.H., Zolensky, M.E., Bernhard, R.P., Warren, J.L., Sapp, C.A., and Dardano, C.B. (1994) LDEF Meteoroid & Debris Special Investigation Group Investigations and Activities at the Johnson Space Center. *LDEF - 69 Months in Space, Third LDEF Post-Retrieval Symposium, NASA CP-3275*, this volume.
- 23) Cour-Palais, B.G. (1987) Hypervelocity Impacts into Metals, Glass, and Composites, *Int. J. Impact Engng.*, 5, p. 225-237.
- 24) Love, S., Brownlee, D.E., King, N.L. and Hörz, F. (1994) Morphology of Meteoroid and Debris Impact Craters Formed in Soft Metal Targets on the LDEF Satellite, Submitted to *Int. J. Impact Engng.*

